

Quantum Recurrent Neural Networks for Dynamical Systems

Yuan Chen
Advisor: Abdul Khaliq



Middle Tennessee State University
PhD Qualifying Exam

August 19, 2024

Contents

1 Introduction

- Qubit and Superposition
- Quantum Gate for Superposition
- Quantum Entanglement

2 Variational Quantum Circuits (VQCs)

3 Models

- Recurrent Neural Networks
- Quantum Recurrent Neural Networks

4 Dynamical Systems

- Numerical Experiment 1: Van der Pol Oscillator
- Numerical Experiment 2: Harmonic Oscillators
- Numerical Experiment 3: Lorenz System

5 Stiff Systems

- Numerical Experiment 4: Radioactive Decay
- Numerical Experiment 5: Stiff Harmonic Oscillators
- Numerical Experiment 6: Robertson System
- Numerical Experiment 7: Plasma System

6 Recent Works and Future Paths

Current Section

1 Introduction

- Qubit and Superposition
- Quantum Gate for Superposition
- Quantum Entanglement

2 Variational Quantum Circuits (VQCs)

3 Models

- Recurrent Neural Networks
- Quantum Recurrent Neural Networks

4 Dynamical Systems

- Numerical Experiment 1: Van der Pol Oscillator
- Numerical Experiment 2: Harmonic Oscillators
- Numerical Experiment 3: Lorenz System

5 Stiff Systems

- Numerical Experiment 4: Radioactive Decay
- Numerical Experiment 5: Stiff Harmonic Oscillators
- Numerical Experiment 6: Robertson System
- Numerical Experiment 7: Plasma System

6 Recent Works and Future Path

Qubit and Superposition

The core distinction between classical and quantum computing lies in their fundamental units of information¹:

The classical computing: bit.

The quantum computing: qubit (quantum binary digit).

Rather than being limited to a strict 0 or 1, a qubit can represent both 0 and 1 simultaneously, as known as superposition.

Superposition is the ability of a quantum system to be in multiple states at the same time until it is measured

1. Jack D. Hidary, Quantum Computing: An applied Approach, *Second Edition*

Qubit and Superposition

- Denote the state $|0\rangle$ as the vector $\begin{pmatrix} 1 \\ 0 \end{pmatrix}$ and the state $|1\rangle$ as the vector $\begin{pmatrix} 0 \\ 1 \end{pmatrix}$.
- The state of a qubit can be described as a linear combination (or superposition) of these basis states:

$$|\psi\rangle = \alpha|0\rangle + \beta|1\rangle$$

- Here, Ψ (or $|\psi\rangle$) represents the overall state of the qubit, which is a superposition of the basis states $|0\rangle$ and $|1\rangle$. The coefficients α and β are complex numbers known as probability amplitudes.

Qubit and Superposition

Theorem 1 (Born's Rule²)

Let a be a quantum-mechanical, has an orthonormal basis of eigenvectors e_i with corresponding eigenvalues λ_i . If the system is in a state Ψ , then the probability $P(a = \lambda_i | \Psi)$ that the eigenvalue λ_i of a is found when a is measured is given by

$$P(a = \lambda_i | \Psi) = |(e_i, \Psi)|^2.$$

In other words, if $\Psi = \sum_i c_i e_i$ (with $\sum_i |c_i|^2 = 1$), then

$$P(a = \lambda_i | \Psi) = |c_i|^2.$$

According to the Born's rule, the probabilities of finding the qubit in either state upon measurement are $|\alpha|^2$ and $|\beta|^2$, with the condition that $|\alpha|^2 + |\beta|^2 = 1$

2. M. Born: Quantenmechanik der Stoszvorgange. Z. Phys. 38, 803-827 (1926)

Quantum Gate for Superposition

- For classical computer, we have Common logic gates include AND, OR, NOT and XOR each performing a specific logical operation for computational tasks.
- Similarly, quantum computing has quantum gates, which manipulate qubits, such as the Hadamard, Pauli-X, Y, Z, and controlled-NOT (CNOT) gates.
- The Hadamard gate acts on a single qubit and transforms it into a superposition of its basis states.

Quantum Gate for Superposition

The Hadamard gate is represented by the following matrix:

$$H = \frac{1}{\sqrt{2}} \begin{pmatrix} 1 & 1 \\ 1 & -1 \end{pmatrix}$$

When the Hadamard gate acts on the state $|0\rangle$:

$$H|0\rangle = \frac{1}{\sqrt{2}} \begin{pmatrix} 1 & 1 \\ 1 & -1 \end{pmatrix} \begin{pmatrix} 1 \\ 0 \end{pmatrix} = \frac{1}{\sqrt{2}} \begin{pmatrix} 1 \\ 1 \end{pmatrix} = \frac{|0\rangle + |1\rangle}{\sqrt{2}}$$

Similarly, when it acts on the state $|1\rangle$:

$$H|1\rangle = \frac{1}{\sqrt{2}} \begin{pmatrix} 1 & 1 \\ 1 & -1 \end{pmatrix} \begin{pmatrix} 0 \\ 1 \end{pmatrix} = \frac{1}{\sqrt{2}} \begin{pmatrix} 1 \\ -1 \end{pmatrix} = \frac{|0\rangle - |1\rangle}{\sqrt{2}}$$

Quantum Entanglement

- **Quantum entanglement** is a phenomenon in which multiple qubits become interconnected in such a way that the state of one qubit cannot be described independently of the state of the other qubits.
- Entanglement can be achieved using a Controlled-NOT (CNOT) gate.
- The operation of the CNOT gate can be described by the following matrix:

$$\text{CNOT} = \begin{pmatrix} 1 & 0 & 0 & 0 \\ 0 & 1 & 0 & 0 \\ 0 & 0 & 0 & 1 \\ 0 & 0 & 1 & 0 \end{pmatrix}$$

Quantum Entanglement

- This operation creates entanglement between the two qubits, which flips the state of the second qubit.
- For example, let's consider applying the CNOT gate to the two-qubit state $|10\rangle$.

Applying the CNOT gate:

$$\text{CNOT} \cdot |10\rangle = \begin{pmatrix} 1 & 0 & 0 & 0 \\ 0 & 1 & 0 & 0 \\ 0 & 0 & 0 & 1 \\ 0 & 0 & 1 & 0 \end{pmatrix} \begin{pmatrix} 0 \\ 0 \\ 1 \\ 0 \end{pmatrix} = \begin{pmatrix} 0 \\ 0 \\ 0 \\ 1 \end{pmatrix} = |11\rangle$$

- More details about quantum information concepts can be found in the paper by Nannicini^{3, 4}.

3. G. Nannicini, An introduction to quantum computing, without the physics, SIAM Rev., 62 (2020), pp. 936–981.

4. G. Nannicini, Giacomo. "Quantum Algorithms for Optimizers." *arXiv* preprint, August 8, 2024.

<https://arxiv.org/abs/2408.07086>.

Current Section

1 Introduction

- Qubit and Superposition
- Quantum Gate for Superposition
- Quantum Entanglement

2 Variational Quantum Circuits (VQCs)

3 Models

- Recurrent Neural Networks
- Quantum Recurrent Neural Networks

4 Dynamical Systems

- Numerical Experiment 1: Van der Pol Oscillator
- Numerical Experiment 2: Harmonic Oscillators
- Numerical Experiment 3: Lorenz System

5 Stiff Systems

- Numerical Experiment 4: Radioactive Decay
- Numerical Experiment 5: Stiff Harmonic Oscillators
- Numerical Experiment 6: Robertson System
- Numerical Experiment 7: Plasma System

6 Recent Works and Future Path

Variational Quantum Circuits (VQCs)

The specific Variational Quantum Circuits (VQCs)^{5, 6}are structured in three main parts:

- Encoding Circuit.
- Variational Circuit.
- Quantum Measurement.

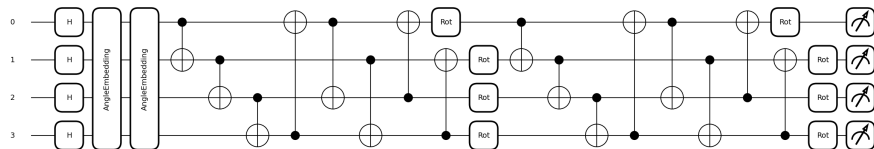


Figure 1: An example of VQC architecture with two layers of entanglements.

5. Mitarai, K., Negoro, M., Kitagawa, M. and Fujii, K., 2018. Quantum circuit learning. *Phys. Rev. A*, 98, 032309.

6. Chen, S.Y.-C., Yang, C.-H.H., Qi, J., Chen, P.-Y., Ma, X. and Goan, H.-S., 2020. Variational quantum circuits for deep reinforcement learning. *IEEE Access*, 8, pp.141007–141024.

Current Section

1 Introduction

- Qubit and Superposition
- Quantum Gate for Superposition
- Quantum Entanglement

2 Variational Quantum Circuits (VQCs)

3 Models

- Recurrent Neural Networks
- Quantum Recurrent Neural Networks

4 Dynamical Systems

- Numerical Experiment 1: Van der Pol Oscillator
- Numerical Experiment 2: Harmonic Oscillators
- Numerical Experiment 3: Lorenz System

5 Stiff Systems

- Numerical Experiment 4: Radioactive Decay
- Numerical Experiment 5: Stiff Harmonic Oscillators
- Numerical Experiment 6: Robertson System
- Numerical Experiment 7: Plasma System

6 Recent Works and Future Path

Deep Learning Models

The Long Short-Term Memory (LSTM) model by Hochreiter and Schmidhuber (1997)⁷ is an enhanced version of recurrent neural networks (RNN) that addresses the issue of capturing long-term dependencies in sequential data.

$$f_t = \sigma(W_f \cdot [h_{t-1}, x_t] + b_f)$$

$$i_t = \sigma(W_i \cdot [h_{t-1}, x_t] + b_i)$$

$$\tilde{C}_t = \tanh(W_C \cdot [h_{t-1}, x_t] + b_C)$$

$$C_t = f_t * C_{t-1} + i_t * \tilde{C}_t$$

$$o_t = \sigma(W_o \cdot [h_{t-1}, x_t] + b_o)$$

$$h_t = o_t * \tanh(C_t)$$

7. Hochreiter, S.; Schmidhuber, J. Long short-term memory. In *Neural Computation*, 1997; 9, 1735–1780.

LSTM

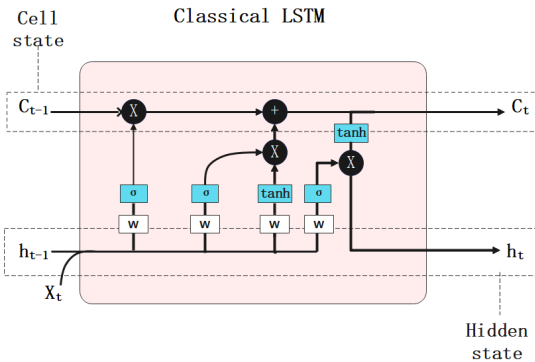


Figure 2: Structure of a single unit of classical LSTM.

GRU

The Gated Recurrent Unit (GRU) is a recurrent neural network architecture that was introduced by Kyunghyun Cho et al.(2014)⁸. It shares similarities with the LSTM model but has a simpler structure with fewer parameters, gates, and equations.

$$z_t = \sigma(W_z \cdot [h_{t-1}, x_t] + b_z)$$

$$r_t = \sigma(W_r \cdot [h_{t-1}, x_t] + b_r)$$

$$\tilde{h}_t = \tanh(W \cdot [r_t * h_{t-1}, x_t] + b)$$

$$h_t = (1 - z_t) * h_{t-1} + z_t * \tilde{h}_t$$

8. Cho, Kyunghyun; van Merriënboer, Bart; Bahdanau, DZmitry; Bougares, Fethi; Schwenk, Holger; Bengio, Yoshua (2014). "Learning Phrase Representations using RNN Encoder-Decoder for Statistical Machine Translation". Association for Computational Linguistics. arXiv:1406.1078.

GRU

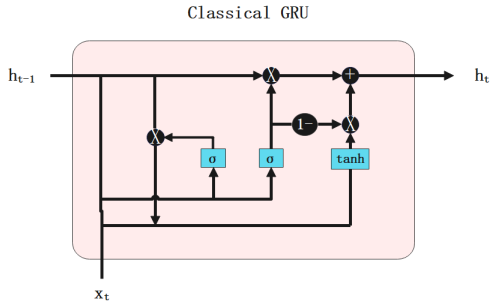


Figure 3: Structure of a single unit of classical GRU.

QLSTM

Quantum Long Short-Term Memory (QLSTM), proposed by Chen et al.(2020)⁹ is a quantum-enhanced version of the traditional LSTM networks integrates with Variational Quantum Circuits (VQCs).

$$f_t = \sigma(\text{VQC1}(v_t))$$

$$i_t = \sigma(\text{VQC2}(v_t))$$

$$\tilde{C}_t = \tanh(\text{VQC3}(v_t))$$

$$c_t = f_t * c_{t-1} + i_t * \tilde{C}_t$$

$$o_t = \sigma(\text{VQC4}(v_t))$$

$$h_t = \text{VQC5}(o_t * \tanh(c_t))$$

$$\tilde{y}_t = \text{VQC6}(o_t * \tanh(c_t))$$

$$y_t = \text{NN}(\tilde{y}_t)$$

9. Chen, S.Y.-C.; Yoo, S.; Fang, Y.-L.L. Quantum Long Short-Term Memory. *Computational Science Initiative, Brookhaven National Laboratory*, 2020.

QLSTM

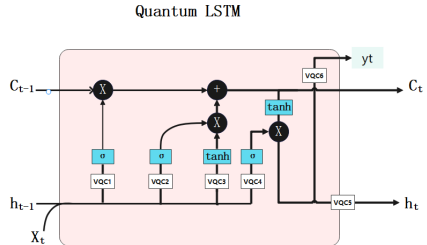
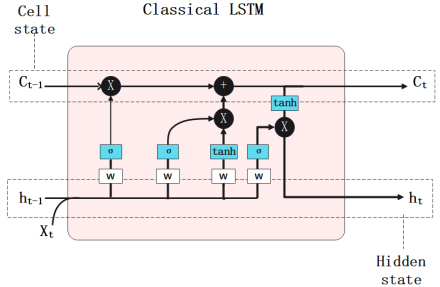


Figure 4: Structure of a single unit of classical LSTM.

Figure 5: Structure of a single unit of QLSTM.

QGRU

Quantum Gated Recurrent Unit (QGRU) by Chen et al.(2020)¹⁰ represents an evolution of traditional GRU networks, integrating with VQCs.

$$r_t = \sigma(\text{VQC1}(v_t))$$

$$z_t = \sigma(\text{VQC2}(v_t))$$

$$o_t = \text{cat}(x_t, r_t * H_{t-1})$$

$$\tilde{H}_t = \tanh(\text{VQC3}(o_t))$$

$$H_t = z_t * H_{t-1} + (1 - z_t) * \tilde{H}_t$$

$$y_t = \text{NN}(H_t)$$

10. Chen, S.Y.-C.; Fry, D.; Deshmukh, A.; Rastunkov, V.; Stefanski, C. Reservoir Computing via Quantum Recurrent Neural Networks. 2020.

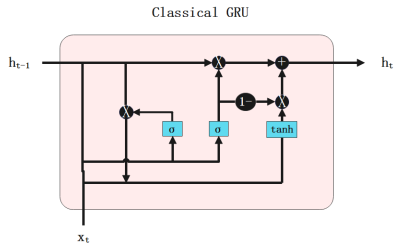


Figure 6: Structure of a single unit of classical GRU.

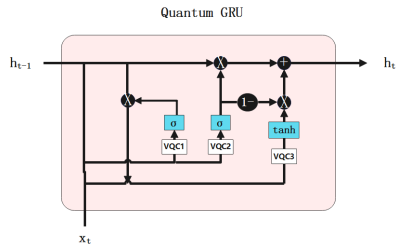


Figure 7: Structure of a single unit of QGRU.

Current Section

1 Introduction

- Qubit and Superposition
- Quantum Gate for Superposition
- Quantum Entanglement

2 Variational Quantum Circuits (VQCs)

3 Models

- Recurrent Neural Networks
- Quantum Recurrent Neural Networks

4 Dynamical Systems

- Numerical Experiment 1: Van der Pol Oscillator
- Numerical Experiment 2: Harmonic Oscillators
- Numerical Experiment 3: Lorenz System

5 Stiff Systems

- Numerical Experiment 4: Radioactive Decay
- Numerical Experiment 5: Stiff Harmonic Oscillators
- Numerical Experiment 6: Robertson System
- Numerical Experiment 7: Plasma System

6 Recent Works and Future Path

Hyperparameter Configuration

Table 1: Hyperparameter Configuration for the First two Experiments.

Hyperparameter	QRNNs Value	RNNs Value
Optimizer	RMSprop	Adam
Loss Function	MSE	MSE
Backend	default.qubit	-
Number of Qubits	4	-
Layer of Entanglements	4	-
Number of Data Points	250	250
Percentage of Train Set	67%	67%
Percentage of Test Set	33%	33%
Epochs	100	100
Learning Rate	0.01	0.01

Numerical Experiment 1¹¹: Van der Pol Oscillator

The oscillator is modeled by the following second-order differential equation:

$$\frac{d^2x}{dt^2} - \mu(1 - x^2) \frac{dx}{dt} + x = 0$$

The parameter μ , representing the nonlinearity and strength of the damping, is set to 1.0 in our simulations.

The initial conditions for the oscillator are chosen as $x_0 = 2.0$ and $y_0 = 0.0$, where x_0 and y_0 represent the initial position and velocity, respectively.

11. Chen, Y.; Khaliq, A. Quantum Recurrent Neural Networks: Predicting the Dynamics of Oscillatory and Chaotic Systems. Algorithms 2024, 17, 163. <https://doi.org/10.3390/a17040163>.

Numerical Experiment 1: Van der Pol Oscillator

To numerically solve the Van der Pol differential equation, we convert it into a system of first-order equations:

$$\begin{aligned}\frac{dx}{dt} &= y, \\ \frac{dy}{dt} &= \mu(1 - x^2)y - x.\end{aligned}$$

The numerical solution is obtained over a time span of 0 to 50 seconds, discretized into 250 time steps.

Numerical Experiment 1: Van der Pol Oscillator

Table 2: Comparison of Train and Test MAE and RMSE for the State of x .

Model	Train MAE	Test MAE	Train RMSE	Test RMSE
LSTM	0.2601	0.2585	0.3002	0.2986
QLSTM	0.1411	0.1397	0.1648	0.1641
GRU	0.1597	0.1591	0.1845	0.1850
QGRU	0.0868	0.0902	0.1013	0.1031

Table 3: Comparison of Train and Test MAE and RMSE for the State of y .

Model	Train MAE	Test MAE	Train RMSE	Test RMSE
LSTM	0.3224	0.3294	0.3737	0.3828
QLSTM	0.1959	0.1851	0.2498	0.2384
GRU	0.3336	0.3375	0.4319	0.4384
QGRU	0.1473	0.1500	0.1931	0.1943

Numerical Experiment 1: Van der Pol Oscillator

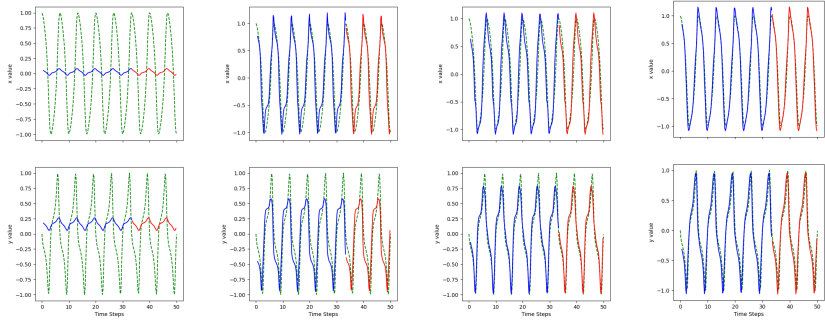


Figure 8: LSTM Predictions Over 100 Epochs for the Van der Pol Oscillator
Up: x, Down: y epoch: 5, 50, 70, 100.

Numerical Experiment 1: Van der Pol Oscillator

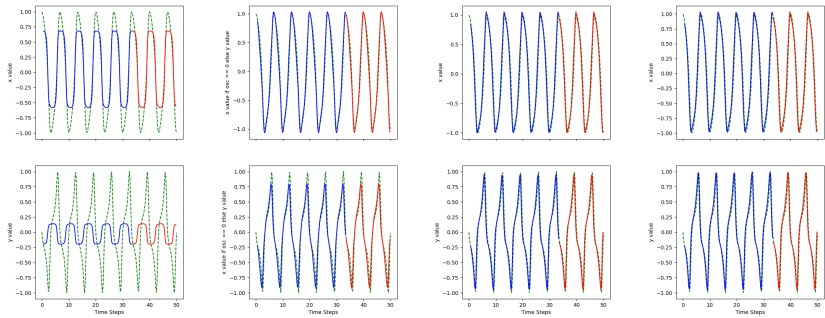


Figure 9: QLSTM Predictions Over 100 Epochs for the Van der Pol Oscillator
Up: x , Down: y epoch: 5, 50, 70, 100.

Numerical Experiment 1: Van der Pol Oscillator

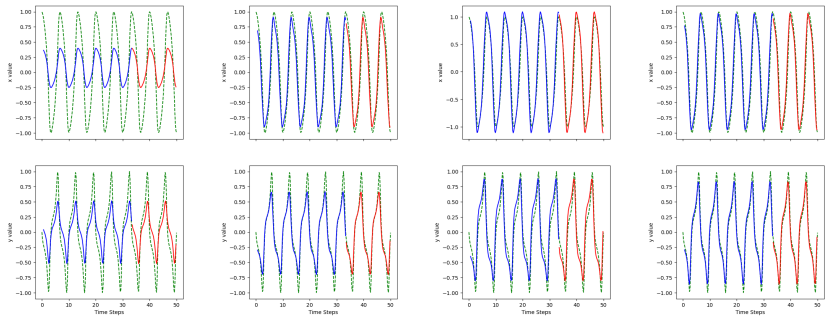


Figure 10: GRU Predictions Over 100 Epochs for the Van der Pol Oscillator
Up: x, Down: y epoch: 5, 50, 70, 100.

Numerical Experiment 1: Van der Pol Oscillator

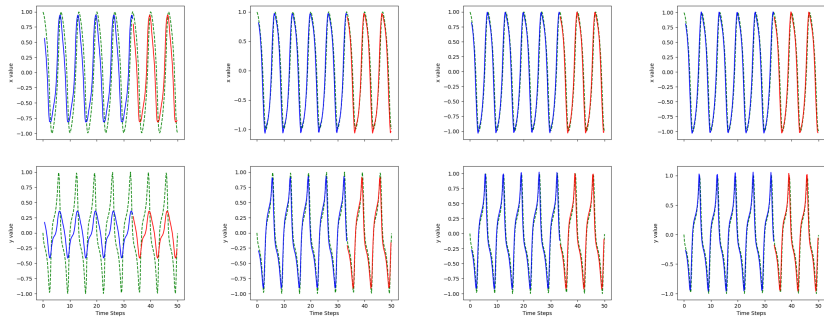


Figure 11: QGRU Predictions Over 100 Epochs for the Van der Pol Oscillator
Up: x, Down: y epoch: 5, 50, 70, 100.

Numerical Experiment 1: Van der Pol Oscillator

Losses over the epochs:

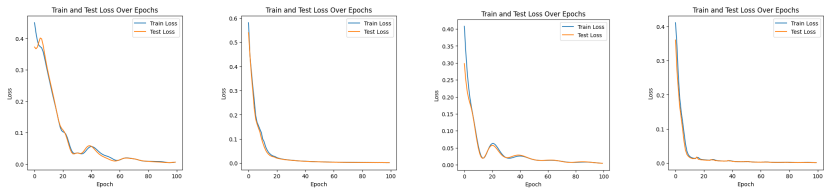


Figure 12: Experiment 1: Train and Test Losses for the Models Over 100 Epochs
From left to right: LSTM, QLSTM, GRU, QGRU.

Numerical Experiment 2: Harmonic Oscillators

The governing differential equations for two coupled damped harmonic oscillators, representing an extended model of the single oscillator, are as follows:

$$\begin{aligned}\frac{d^2\theta_1}{dt^2} &= -\frac{b_1}{m_1} \frac{d\theta_1}{dt} - \frac{g}{l_1} \sin(\theta_1) + \frac{k_c}{m_1} (\theta_2 - \theta_1), \\ \frac{d^2\theta_2}{dt^2} &= -\frac{b_2}{m_2} \frac{d\theta_2}{dt} - \frac{g}{l_2} \sin(\theta_2) + \frac{k_c}{m_2} (\theta_1 - \theta_2).\end{aligned}$$

Here:

$g = 9.81 \text{ m/s}^2$, $b_1 = b_2 = 0.15$, $l_1 = l_2 = 1.0 \text{ m}$, $m_1 = m_2 = 1.0 \text{ kg}$, and $k_c = 0.05$ define the system's characteristics. The initial conditions are set with angular displacements $\theta_1 = \theta_2 = 0$ and angular velocities $\dot{\theta}_1 = 3.0$, $\dot{\theta}_2 = 0.0 \text{ rad/sec}$.

Numerical Experiment 2: Harmonic Oscillators

Table 4: Comparison of Train and Test MAE and RMSE for Oscillator 1.

Model	Train MAE	Test MAE	Train RMSE	Test RMSE
LSTM	0.5467	0.4371	0.7761	0.4922
QLSTM	0.5284	0.4763	0.6987	0.5374
GRU	0.3648	0.4396	0.4499	0.4941
QGRU	0.2585	0.2411	0.3587	0.2701

Table 5: Comparison of Train and Test MAE and RMSE for Oscillator 2.

Model	Train MAE	Test MAE	Train RMSE	Test RMSE
LSTM	0.2190	0.3597	0.2814	0.4248
QLSTM	0.1244	0.2591	0.1607	0.2885
GRU	0.1160	0.0858	0.1483	0.1006
QGRU	0.0794	0.0482	0.0949	0.0602

Numerical Experiment 2: Harmonic Oscillators

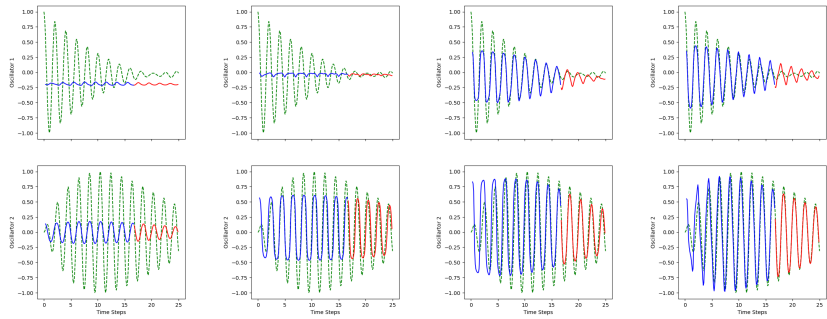


Figure 13: LSTM Predictions Over 100 Epochs

Up: Oscillator 1, Down: Oscillator 2 epoch: 5, 50, 70, 100.

Numerical Experiment 2: Harmonic Oscillators

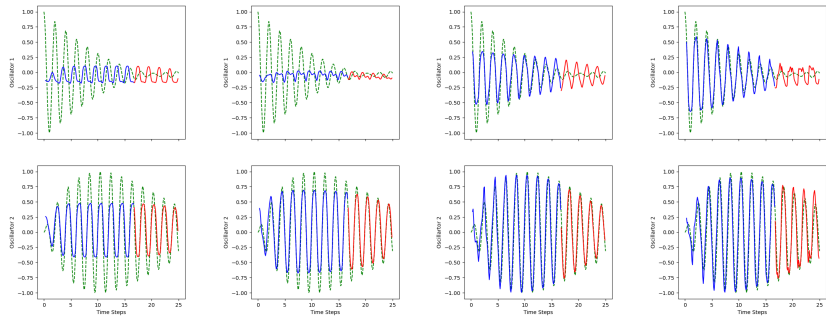


Figure 14: QLSTM Predictions Over 100 Epochs
Up: Oscillator 1, Down: Oscillator 2 epoch: 5, 50, 70, 100.

Numerical Experiment 2: Harmonic Oscillators

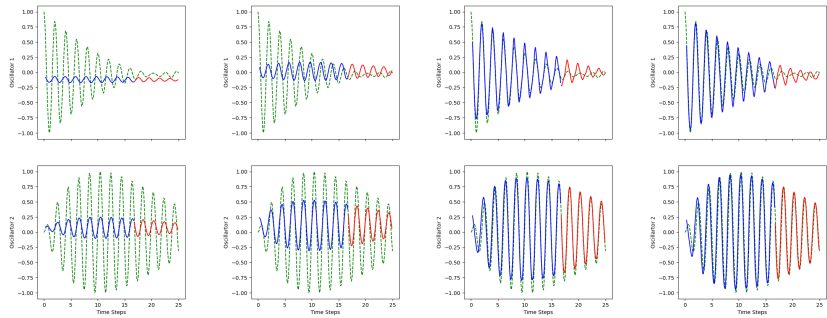


Figure 15: GRU Predictions Over 100 Epochs

Up: Oscillator 1, Down: Oscillator 2 epoch: 5, 50, 70, 100.

Numerical Experiment 2: Harmonic Oscillators

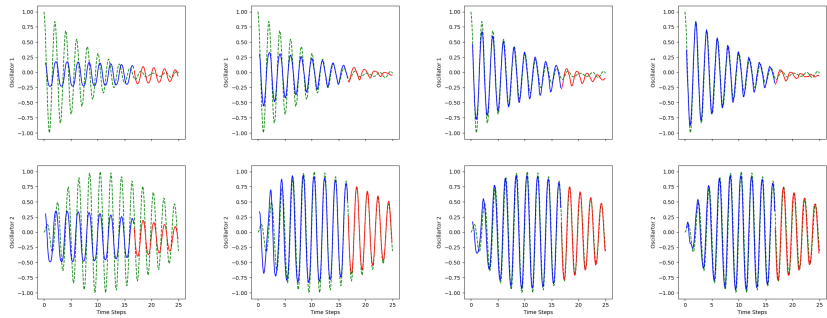


Figure 16: QGRU Predictions Over 100 Epochs
Up: Oscillator 1, Down: Oscillator 2 epoch: 5, 50, 70, 100.

Numerical Experiment 2: Harmonic Oscillators

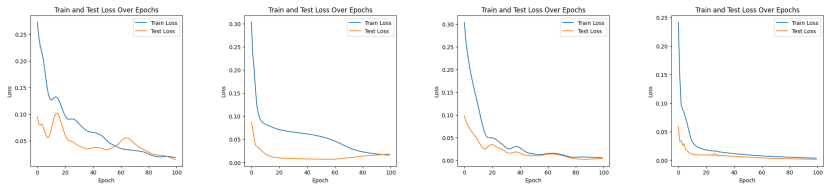


Figure 17: Experiment 2: Train and Test Losses for the Models Over 100 Epochs

From left to right: LSTM, QLSTM, GRU, QGRU.

Numerical Experiment 3: Lorenz System

The Lorenz equations, fundamental in chaos theory, model the dynamics of atmospheric convection and are characterized by their chaotic nature for certain parameter values. The system is described by:

$$\begin{aligned}\frac{dx}{dt} &= \sigma(y - x), \\ \frac{dy}{dt} &= x(\rho - z) - y, \\ \frac{dz}{dt} &= xy - \beta z.\end{aligned}$$

Here, x , y , and z represent the system states, and the chosen values $\sigma = 10.0$, $\beta = \frac{8}{3}$, and $\rho = 28.0$

Numerical Experiment 3: Lorenz System

Table 6: Mean Absolute Error (MAE) for Each State on Test Set.

Model	X	Y	Z
LSTM	2.0361	2.1232	2.2119
QLSTM	0.8820	0.9473	1.0206
GRU	1.1684	1.1719	1.1710
QGRU	0.4864	0.4723	0.4555

Table 7: Root Mean Square Error (RMSE) for Each State on Test Set.

Model	X	Y	Z
LSTM	2.1736	2.2718	2.3714
QLSTM	1.2234	1.2723	1.3348
GRU	1.1783	1.1748	1.1740
QGRU	0.4971	0.4846	0.4745

Numerical Experiment 3: Lorenz System

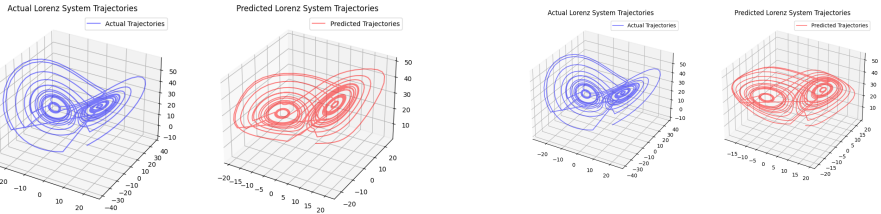


Figure 18: Predicted Lorenz System Trajectory by LSTM Model.

Figure 19: Predicted Lorenz System Trajectory by QLSTM Model.



Figure 20: Predicted Lorenz System Trajectory by GRU Model.

Figure 21: Predicted Lorenz System Trajectory by QGRU Model.

Numerical Experiment 3: Lorenz System

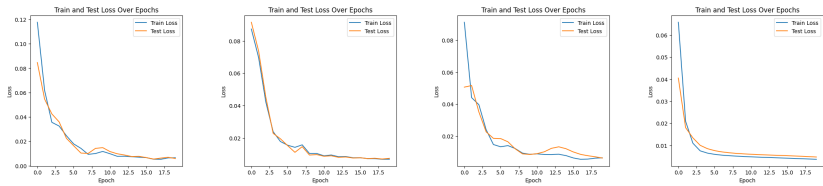


Figure 22: Experiment 3: Train and Test Losses for the Models Over 20 Epochs
From left to right: LSTM, QLSTM, GRU, QGRU.

Current Section

1 Introduction

- Qubit and Superposition
- Quantum Gate for Superposition
- Quantum Entanglement

2 Variational Quantum Circuits (VQCs)

3 Models

- Recurrent Neural Networks
- Quantum Recurrent Neural Networks

4 Dynamical Systems

- Numerical Experiment 1: Van der Pol Oscillator
- Numerical Experiment 2: Harmonic Oscillators
- Numerical Experiment 3: Lorenz System

5 Stiff Systems

- Numerical Experiment 4: Radioactive Decay
- Numerical Experiment 5: Stiff Harmonic Oscillators
- Numerical Experiment 6: Robertson System
- Numerical Experiment 7: Plasma System

6 Recent Works and Future Path

Stiff Dynamical Systems

Consider a system of ODEs given by:

$$\frac{d\mathbf{y}}{dt} = \mathbf{f}(\mathbf{y}, t),$$

where \mathbf{y} is the vector of dependent variables, and \mathbf{f} is a vector-valued function describing the rate of change of \mathbf{y} with respect to time t . Stiffness is characterized by the presence of eigenvalues with vastly different magnitudes.

Stiff Dynamical Systems

The Jacobian matrix of the system, which provides insight into the local behavior of the system, is defined as:

$$\mathbf{J} = \frac{\partial \mathbf{f}}{\partial \mathbf{y}},$$

where \mathbf{J} is the matrix of partial derivatives of \mathbf{f} with respect to \mathbf{y} . The eigenvalues λ_i of the Jacobian matrix \mathbf{J} determine the system's stiffness. The stiffness ratio, R , is defined as:

$$R = \frac{|\lambda_{\max}|}{|\lambda_{\min}|},$$

A high stiffness ratio (usually greater than 1000) indicates severe stiffness.

Numerical Experiment 4: Radioactive Decay

Radioactive decay, which is a process that can be described by a differential equation, capturing the rate at which a quantity of radioactive material decreases over time. The rate of change of the number of radioactive atoms, N , can be modeled using the following ODE:

$$\frac{dN}{dt} = -\lambda_1 N - \lambda_2 N^2,$$

Where, λ_1 is set to 0.1, representing the rate of the first process, while λ_2 is set to 50.0, representing the rate of the second process.

Table 8: Comparison of QLSTM and LSTM on Radioactive Decay

Metric	QLSTM		LSTM	
	Train	Test	Train	Test
MAE	10.1528	1.8403	25.7313	11.9552
RMSE	12.0770	1.8637	33.8402	11.9576

Numerical Experiment 4: Radioactive Decay

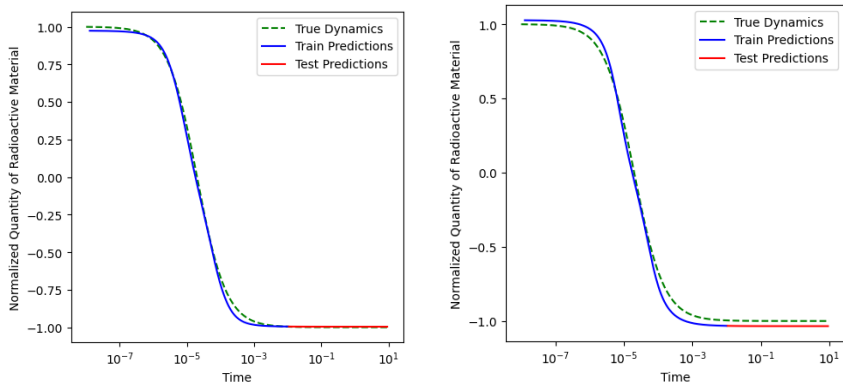


Figure 23: Experiment 4: Predictions QLSTM (left) vs LSTM (right), Train (blue) vs Test (red)

Numerical Experiment 4: Radioactive Decay

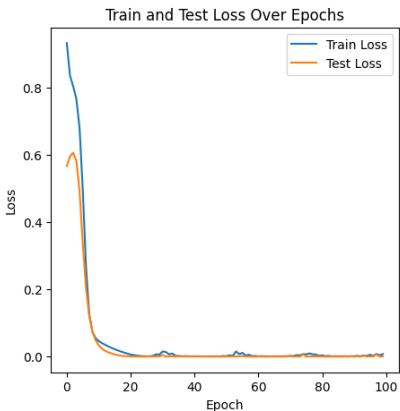
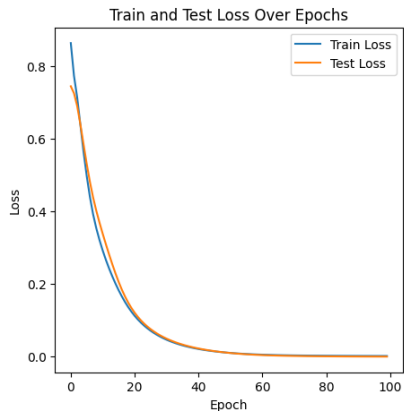


Figure 24: Experiment 4: Loss over 100 epochs QLSTM (left) vs LSTM (right), Train (blue) vs Test (orange)

Numerical Experiment 5: Stiff Harmonic Oscillators

The stiff harmonic system is defined as following:

$$\frac{d\theta_1}{dt} = \omega_1,$$

$$\frac{d\omega_1}{dt} = -\frac{b_1}{m_1}\omega_1 - \frac{g}{l_1}\sin(\theta_1) + \frac{k_c}{m_1}(\theta_2 - \theta_1),$$

$$\frac{d\theta_2}{dt} = \omega_2,$$

$$\frac{d\omega_2}{dt} = -\frac{b_2}{m_2}\omega_2 - \frac{g}{l_2}\sin(\theta_2) + \frac{k_c}{m_2}(\theta_1 - \theta_2).$$

The damping factors for the two oscillators, b_1 and b_2 , are set to 200.0 and 0.1, respectively. The coupling constant k_c is set to 100.0.

Numerical Experiment 5: Stiff Harmonic Oscillators

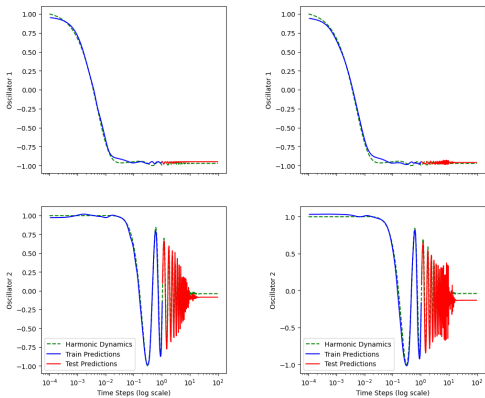


Figure 25: Experiment 5: Two Coupled Damped Harmonic Oscillators: Predictions QLSTM (left) vs LSTM (right), Top: Oscillator 1, Bottom: Oscillator 2

Numerical Experiment 5: Stiff Harmonic Oscillators

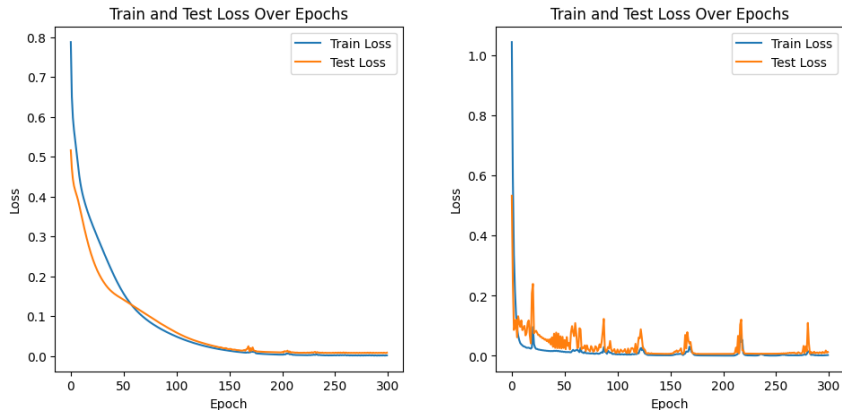


Figure 26: Experiment 5: Two Coupled Damped Harmonic Oscillators: Loss over 300 epochs QLSTM (left) vs LSTM (right), Train (blue) vs Test (orange)

Numerical Experiment 6: Robertson System

The Robertson system consists of three coupled nonlinear differential equations given by:

$$\frac{dy_1}{dt} = -0.04y_1 + 10^4 y_2 y_3,$$

$$\frac{dy_2}{dt} = 0.04y_1 - 10^4 y_2 y_3 - 3 \times 10^7 y_2^2,$$

$$\frac{dy_3}{dt} = 3 \times 10^7 y_2^2,$$

where $y_1(t)$, $y_2(t)$, and $y_3(t)$ represent the concentrations of different chemical species over time.

The initial conditions for the system are:

$$y_1(0) = 1, \quad y_2(0) = 0, \quad y_3(0) = 0.$$

Numerical Experiment 6: Robertson System

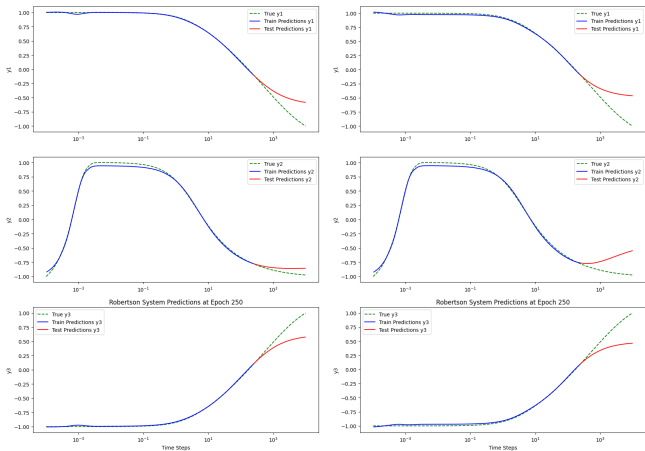


Figure 27: Experiment 6: Predictions QLSTM (left) vs LSTM (right), Train (blue) vs Test (red), Top: y_1 , Middle: y_2 , Bottom: y_3

Numerical Experiment 6: Robertson System

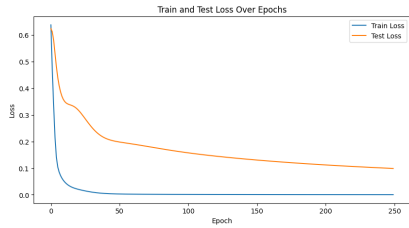
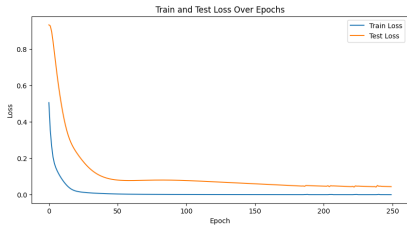


Figure 28: Experiment 6: Loss over 250 epochs QLSTM vs LSTM, Train (blue) vs Test (orange).

Numerical Experiment 7: Plasma System

The system of differential equations describing the plasma dynamics is:

$$\frac{dv_e}{dt} = -\frac{e}{m_e} E - v_e v_e,$$

$$\frac{dv_{i1}}{dt} = \frac{e}{m_{i1}} E - v_{i1} v_{i1},$$

$$\frac{dv_{i2}}{dt} = \frac{e}{m_{i2}} E - v_{i2} v_{i2},$$

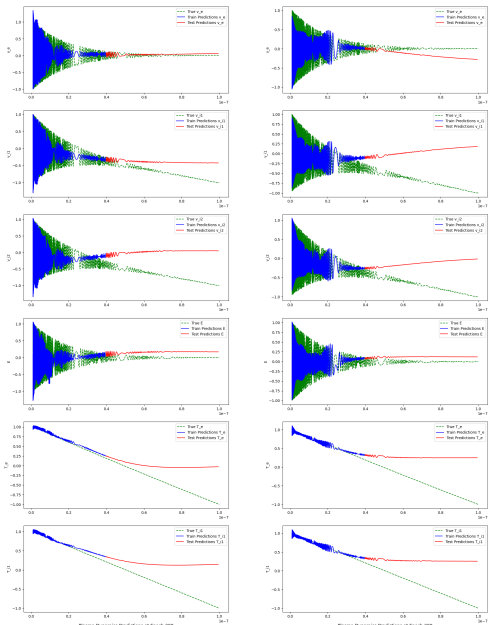
$$\frac{dE}{dt} = -\frac{e}{\epsilon_0} (n_{i1} v_{i1} + n_{i2} v_{i2} - n_e v_e),$$

$$\frac{dT_e}{dt} = -\gamma_e T_e,$$

$$\frac{dT_{i1}}{dt} = -\gamma_{i1} T_{i1},$$

$$\frac{dT_{i2}}{dt} = -\gamma_{i2} T_{i2},$$

Numerical Experiment 7: Plasma System



Numerical Experiment 7: Plasma System

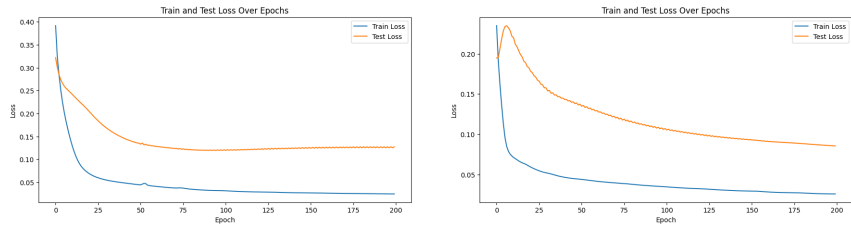


Figure 30: Experiment 7: Loss over 200 epochs QLSTM (left) vs LSTM (right).

Current Section

1 Introduction

- Qubit and Superposition
- Quantum Gate for Superposition
- Quantum Entanglement

2 Variational Quantum Circuits (VQCs)

3 Models

- Recurrent Neural Networks
- Quantum Recurrent Neural Networks

4 Dynamical Systems

- Numerical Experiment 1: Van der Pol Oscillator
- Numerical Experiment 2: Harmonic Oscillators
- Numerical Experiment 3: Lorenz System

5 Stiff Systems

- Numerical Experiment 4: Radioactive Decay
- Numerical Experiment 5: Stiff Harmonic Oscillators
- Numerical Experiment 6: Robertson System
- Numerical Experiment 7: Plasma System

6 Recent Works and Future Paths

Works Summary

- **Paper:** Chen, Y.; Khaliq, A. Quantum Recurrent Neural Networks: Predicting the Dynamics of Oscillatory and Chaotic Systems. Algorithms 2024, 17, 163. <https://doi.org/10.3390/a17040163>.
- **Paper:** Quantum Long Short-Term Memory Networks for Stiff Dynamical Systems. Submitted to Applied Soft Computing.
- **Conference Presentation:** "Enhancing Dynamical System Analysis Through Quantum Recurrent Neural Networks." 2024. In 2024 Society for Industrial and Applied Mathematics (SIAM) Annual Meeting (AN24), Spokane, WA, July 8-12.

Current Research: VQA: Application in Fractional Order of PDE

This study is inspired by the study by Leong et al.¹². First, we recall the definition of the Caputo fractional derivative:

$$D_t^\alpha u(t, x) = \frac{1}{\Gamma(n-\alpha)} \int_0^t \frac{\partial^n u(s, x)}{\partial s^n} \frac{ds}{(t-s)^{\alpha-n+1}},$$

where Γ denotes the Gamma function and $0 < \alpha < 1$ is the fractional order.

12. Fong Yew Leong, Dax Enshan Koh, Jian Feng Kong, Siong Thye Goh, Jun Yong Khoo, Wei-Bin Ewe, Hongying Li, Jayne Thompson, Dario Poletti; Solving fractional differential equations on a quantum computer: A variational approach. AVS Quantum Sci. 1 September 2024; 6 (3): 033802. <https://doi.org/10.1116/5.0202971>

VQA: Application in Fractional Order of PDE

By the first-order finite difference approximation of the Caputo derivative of order $0 < \alpha \leq 1$ is used:

$$D_t^\alpha u(t_k, x_n) \approx g_{\alpha, \tau} \sum_{j=1}^k w_j^{(\alpha)} (u_{k-j+1}^n - u_{k-j}^n),$$

where $u_k^n = u(t_k, x_n)$, $g_{\alpha, \tau} = \tau^{-\alpha} / \Gamma(2 - \alpha)$, and $w_j^{(\alpha)} = j^{1-\alpha} - (j-1)^{1-\alpha}$.

VQA: Application in Fractional Order of PDE

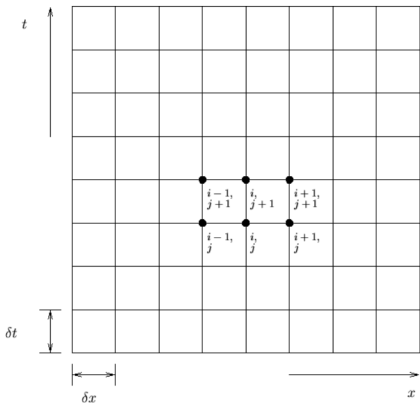


Figure 31: PDE Mesh

VQA: Application in Fractional Order of PDE

Variational Quantum Algorithm (VQA):

Step 1: Initial $|u_0\rangle$, r_0 and θ_0 .

Step 2: Find $|f_{k-1}\rangle$, where

$$|\tilde{f}_{k-1}\rangle = w_k r_0 |u_0\rangle - \sum_{j=1}^{k-1} \Delta w_j r_{k-j} |u_{k-j}\rangle,$$

VQA: Application in Fractional Order of PDE

Step 3: Prepare ansatz u_k (normalized $|\tilde{u}_k\rangle$) at time step k , with initial r_k and θ_k , where

$$|u_k\rangle := \prod_{i=1}^l W_{l-i+1} R(\theta_{k,l-i+1}) |0\rangle,$$

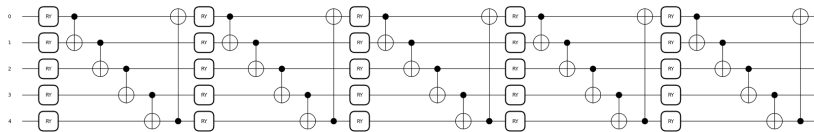


Figure 32: A 5 qubits 5 layers Ansatz

VQA: Application in Fractional Order of PDE

Step 4: The cost function (loss function) is defined ¹³:

$$C_k(\theta_k) = -\frac{1}{2} \left(\frac{\langle u_k | \tilde{f}_{k-1} \rangle^2}{\langle u_k | A | u_k \rangle} \right).$$

Step 5: Measure $\langle u_k | \tilde{f}_{k-1} \rangle$ and $\langle u_k | A | u_k \rangle$ with some quantum circuits.

Step 6: Use some classical optimizer to find r_k and θ_k .

Step 7: Updated $|\tilde{u}_k\rangle$.

$$|\tilde{u}_k\rangle := r_k \prod_{i=1}^I W_{I-i+1} R(\theta_{k,I-i+1}) |0\rangle,$$

¹³ki Sato, Ruho Kondo, Satoshi Koide, Hideki Takamatsu, and Nobuyuki Imoto. Variational quantum algorithm based on the minimum potential energy for solving the Poisson equation. Physical Review A, 104(5):052409, 2021.

Future Works

- Deeper model featuring more layers and more complex structure.
- Quantum computer instead of default simulator.
- Quantum graph neural networks (QGNN)¹⁴.
- Physics-Informed structure (QPIRNN).
- Quantum based Kolmogorov-Arnold Networks (QKAN)¹⁵.
- Application in large system of PDE¹⁶.
- Portfolio optimization¹⁷.

14. Verdon, Guillaume, Trevor McCourt, Enxhell Luzhnica, Vikash Singh, Stefan Leichenauer, and Jack Hidary. 2019. "Quantum Graph Neural Networks." *arXiv preprint*, September 26, 2019. <https://arxiv.org/abs/1909.12223>.

15. Liu, Ziming, Yixuan Wang, Sachin Vaidya, Fabian Ruehle, James Halverson, Marin Soljačić, Thomas Y. Hou, and Max Tegmark. "KAN: Kolmogorov-Arnold Networks." Massachusetts Institute of Technology, California Institute of Technology, Northeastern University, and The NSF Institute for Artificial Intelligence and Fundamental Interactions.

16. Hyde, David, and Alex Pothen. "An Introduction to Quantum Computing and Applied Mathematics." *SIAM News* 57, no. 3 (April 2024). <https://www.siam.org/publications/siam-news/articles/an-introduction-to-quantum-computing-and-its-applications>

17. Jacquier, Antoine, Oleksiy Kondratyev, Gordon Lee, and Mugad Oumgari. "Quantum Computing for Financial Mathematics." *SIAM News* 57, no. 3 (April 2024). <https://www.siam.org/publications/siam-news/articles/quantum-computing-for-financial-mathematics>

Multumesc Ua Tsaug Rau Koj
Dank Je Mochchakkeram
Chokrane Maake **CHOKRANE**
Kiitos Kiitos Juspaaxar

Nirringrazzjak Terma Kasih Matondo
Raibh Maith Agat Chokrane Kiitos
Grazie Maake Dankon Obrigado
Terma Kasih Thank You Obrigado
Asante Obrigado

Dank Je Asante Obrigado
Kiitos Obrigado
Merci Obrigado
Thank You Obrigado
Asante Obrigado

Nirringrazzjak Salamat Obrigado
Mochchakkeram Salamat Obrigado
Multumesc Salamat Obrigado
Spasibo Salamat Obrigado
Cam on ban Salamat Obrigado

Mochchakkeram Juspaaxar

Mamana THANK YOU **OBRIGADO**

© dreamtime.com